

Progress Report for year 1 covering the period
July 1, 1999 – June 30, 2000

Mechanism of Irradiation Assisted Cracking of Core Components in Light Water Reactors

Grant #DE-FG07-99ID13768
University of Michigan

Gary S. Was, PI
Michael Atzmon, co-PI
Lumin Wang, co-PI
Jeremy Busby
Benjamin Grambau

The degradation of mechanical properties known as irradiation-assisted stress corrosion cracking (IASCC) has been occurring for at least 20 years in nuclear-reactor core components made of austenitic iron- and nickel-base alloys. It is becoming increasingly evident that the problem is widespread without regard to environment or material composition and tens or hundreds of core components may be susceptible to this form of degradation. However, little is known about the specific mechanisms that control cracking susceptibility. During irradiation, materials experience changes to the microstructure (such as the formation of voids and dislocation loops cause hardening) and changes to the local composition (radiation-induced segregation (RIS) at grain boundaries). Both microstructural effects and microcompositional effects increase with increasing radiation damage and have been identified as possible mechanisms for IASCC; however, the exact role that each plays in IASCC is unclear.

High temperature annealing treatments have been successful in eliminating microstructural and microchemical changes altogether, while lower temperature anneals have been found to partially remove these features^{1,2,3}. Potentially, an annealing condition may be found such that either microstructural or microchemical damage is removed entirely, while the other remains unaffected, thus allowing for the role of one effect to be isolated.

The primary objective of this program is isolate both radiation damage features and determine their roles in IASCC independently and synergistically. If one feature can be removed preferentially, then the influence of the remaining irradiation-induced effect on IASCC can be examined. This program is conducted using proton irradiation as the radiation damage tool. Previous work has shown that proton irradiation is extremely effective in simulating LWR core irradiation in stainless steel alloys. The program is divided into two parts; the isolation of microchemistry and isolation of microstructure. The first is accomplished by post-irradiation annealing (PIA), and the second by controlling the irradiation conditions. The bulk of the progress in year one has been in the development of post-irradiation annealing conditions to isolate RIS by selectively removing the dislocation loop microstructure. Initial experiments on creating a loop microstructure without RIS have also been performed.

PHASE 1: ION SOURCE UPGRADE

Phase 1 consists of the specification, ordering, delivery and acceptance of the TORVIS ion source from National Electrostatics Corporation. The new source will provide greater beam current and higher reliability than does our current source. The order for the source was placed on October 10, 1999. The delivery time indicated in the quote was to be 6 months from the receipt of order, but upon receipt of the order, the company required 8 months, resulting in a June 1, 2000 delivery date. In May we learned that due to the loss of two staff at NEC, the

source delivery was going to be delayed. A revised delivery date was not specified by the company, but it appears that delivery in July is very likely. The 5 month delay was caused by three factors, 1) 1 months required to negotiate a purchasing agreement with NEC, 2) a longer delivery time required by NEC (2 months), and 3) a delayed delivery schedule on the part of NEC (2 months). Thus, the delivery and installation of this source will occur in the second year of the program.

PHASE 2: MICROCHEMISTRY AND MICROSTRUCTURE – PROOF OF PRINCIPLE

Post-Irradiation Annealing to Isolate RIS

Activities in this part of the program consisted of modeling the evolution of dislocation loops and RIS during post-irradiation annealing and experiments to determine the proper time-temperature conditions where RIS can be effectively isolated.

Modeling

Prior to experiments, the behavior of microstructural and microchemical changes during post-irradiation annealing was investigated using model simulations. Simulation over a wide range of temperature and time combinations was used as a guideline in planning initial annealing experiments.

A simple model was developed to simulate of the annealing of dislocation loops. During low temperature annealing, interstitial populations are negligible. Thus, only vacancies will interact with dislocation loop populations, which are predominantly interstitial in nature. As vacancies are absorbed at interstitial dislocation loops during annealing, the loops shrink. The rate at which vacancies are absorbed was estimated as follows:

$$\text{Rate of thermal Vacancy capture} = \frac{2 \pi D_v \rho_d C_v}{\ln (R/R_d)}, \quad (1)$$

where D_v is the vacancy diffusivity, ρ_d is the dislocation density, C_v is the vacancy concentration, R is the radius of the capture volume, and R_d is the capture radius of the dislocation loop. After determining the rate of vacancy capture, the size of the loop can be calculated at any time during an anneal by calculating the number of vacancies that have been absorbed. The measured loop density and radius resulting from a 1.0 dpa irradiation of a high-purity 304L stainless steel sample at 360°C was used as the starting condition for a series of simulations over a wide range of times and temperatures.

There are several limitations to this very simple model. This model does not account for the change in vacancy absorption rate with changing loop radius, or the influence of stacking fault energy or line energy of the loop, both of which influence the vacancy concentration at the loop. Further, the size distribution of the loop population is not considered. Finally, this simple model yields only the size of the average loop during annealing but not more easily measurable physical quantities such as hardness or changes in yield stress. Future revisions of the model will account for these deficiencies.

The modified-inverse Kirkendall (MIK) model developed by Allen⁴ was used to simulate the behavior of RIS during post-irradiation annealing. The MIK model, an improvement on the Perks model⁵, was originally designed to simulate the development of RIS during irradiation for a ternary alloy. In this work, the model was first used to simulate the RIS profile resulting from a 1.0 dpa irradiation at 360°C of the HP-304L alloy used in the microstructure model. For annealing (i.e. displacement rate = 0), the MIK model used the segregation profile resulting from

the 1.0 dpa irradiation as the initial condition for a series of anneals over the same time-temperature combinations used in the microstructure model.

The simulation results for both models are compared in Figure 1 over a wide range of temperatures (400°C to 600°C) and times (1 to 10⁷ seconds). The simulations indicate that the dislocation loops (left) are removed faster than is RIS (right). Further, there appear to be regimes in time-temperature space where the dislocation loops are completely removed and RIS is largely unaffected. The simulation results for an isothermal anneal at 500°C are shown in Figure 2, along with existing experimental data from neutron irradiations¹, for the amount of chromium depletion, ΔCr and the dislocation line length, D_L remaining after heat treatment. The simulations are in good agreement with the experimental results that provide verification of the existence of such an annealing condition.

Using the annealing simulations as a guideline, a series of annealing experiments have been conducted. Both a high-purity 304L and a commercial-purity 304 stainless steel alloy have been examined. Samples of each alloy were irradiated with 3.2 MeV protons to 1.0 dpa at 360°C. Following irradiation, the irradiated hardness, dislocation microstructure and radiation segregation profiles were measured. Post-irradiation anneals on the HP-304L were then performed at 500°C for 45 minutes, 500°C for 300 minutes, 550°C for 45 minutes, 600°C for 45 minutes, 600°C for 90 minutes, and 650°C for 45 minutes. Anneals of the CP-304 were done at 400°C for 45 minutes, 450°C for 45 minutes, 500°C for 45 minutes, 600°C for 90 minutes, and 650°C for 45 minutes. Following annealing, the irradiated hardness, dislocation microstructure and radiation segregation profiles were again measured and compared to the as-irradiated measurements.

The percentage of the as-irradiated hardness following annealing for both alloys is plotted in Figure 3 as a function of iron diffusion distance. The iron diffusion distance serves as a single variable to allow for the comparison of different time-temperature combinations. The iron diffusion distance is defined as follows:

$$\text{Fe Diffusion Distance} = \sqrt{(D_{Fe} t)} \quad , \quad (2)$$

where D_{Fe} is the diffusivity of iron (a function of annealing temperature) and t is the annealing time. Published data from post-irradiation experiments on similar alloys are also plotted in Figure 2 and are in excellent agreement with those from this study. Unfortunately, the very simple model does not allow for a prediction of the hardness during annealing.

Changes in the total loop line length (circumference of average loop x loop density) during annealing are plotted as a function of diffusion distance in Figure 4 with the existing literature data. In addition, the model prediction for the microstructure is plotted. The simulation results are in poor agreement with both sets of experimental data. This is probably due to the deficiencies in the simple model as listed earlier. The effects of change in vacancy absorption with changing loop radius, line energy and stacking fault energy would all result in loops being more rapidly removed during simulation than actual annealing, all of which would provide a better fit to the data in Fig. 4. Future improvements to the microstructure annealing model are expected to reduce the difference between model and experimental results.

The annealing behavior of grain boundary Cr composition is shown in Figure 5, with existing data from the open literature and the model simulation. The comparison between the data from this study and other experiments is quite good, as is the comparison between the simulation prediction and all data sets for shorter Fe diffusion distances. At higher diffusion distances (higher annealing temperatures or longer annealing times), the model overestimates the amount of RIS remaining. This may be due to a synergy between irradiated microstructure and segregation profiles during annealing. As the dislocation loops are removed, there are fewer

sites competing with grain boundaries for vacancies. Thus, as the dislocation population is removed, there will be an acceleration of the RIS profile removal. This possible synergy will be investigated.

The data trend lines shown in Figures 3-5, are plotted together in Figure 6 and clearly show that the irradiated microstructure and hardening are removed preferentially to the grain boundary segregation for sufficiently small Fe diffusion distances. This is consistent with both the simulation results and existing data from other post-irradiation annealing experiments. The annealing results at a diffusion distance of 0.0016 cm (600°C for 90 minutes) are of interest. Following this annealing treatment for the HP-304L alloy, the radiation-induced hardening and dislocation population have been virtually eliminated while over 80% of the grain boundary Cr depletion remains. In the CP-304 alloy, all the hardening has been removed. Dislocation density and RIS have not yet been measured in this alloy.

By determining the cracking susceptibility in annealed samples where only RIS remains and comparing this result to the as-irradiated susceptibility, the exact role of RIS in IASCC can be determined. Work on this part of the project (Phase 3) in the second year will concentrate on quantifying the microstructure and microchemistry in the annealing time-temperature regimes that span the greatest separation of RIS and loop line length. In Phase 4 of the project, we will also conduct IASCC experiments in normal water chemistry to determine the relationship between RIS/microstructure and IASCC.

Controlled Irradiation to Isolate the Radiation Damage Microstructure

The second part of this project involves the formation of the radiation damage microstructure without accompanying RIS. This is being pursued initially by low-temperature irradiation followed by post-irradiation annealing. Irradiation at low temperature will suppress long range diffusion required for RIS and the development of a dislocation loop population. Instead, the as-irradiated microstructure consists of a high density of damage zones and loop nuclei. Post-irradiation annealing may be effective in growing the loop population and size distribution to a point where it becomes similar to that created by irradiation at reactor temperatures. The objective of work in the first year is to begin determination of whether such an approach can produce the desired microstructure with no RIS.

Experiment

In order to separate the effect of microstructure and microchemistry a series of low-temperature irradiations are being performed. Typical proton irradiations to simulate LWR irradiation effects are conducted at 360°C to produce both a defect dislocation structure (microstructure) and RIS of major alloying elements and impurities (microchemistry). Low-temperature irradiation (50°C) suppresses RIS and provides a somewhat similar microstructure. A series of post-irradiation annealing experiments will attempt to tailor the microstructure to match that under irradiation at 360°C.

The first irradiation at 323°K was completed in late December 1999 to a dose of 0.3 dpa on a commercial purity (CP) 304L austenitic stainless steel. Based on an extensive literature review of comparable neutron data, this irradiation will likely produce a high density ($5 \times 10^{24}/\text{m}^3$) of small (0.5-2 nm) defect clusters (mostly vacancy type) with no RIS. Quantification of the microstructure is complicated by the small size of the damage zones. However, we are in the final stages of installation of a JEOL 2010F FEG-STEM which will provide the best available capability for imaging these defects. A measure of the microstructure effect is the hardness. The hardness of the as-irradiated structure was measured using a Vickers hardness indenter with a 25 g load. Results showed an increase of approximately $\Delta H_v = 85 \text{ kg/mm}^2$. This compares with a

value of about 60 kg/mm² following an irradiation at 360°C to 1.0 dpa. These results are encouraging as they support a very high density of very small defect clusters. Microchemical analysis by FEG-STEM of an the as-irradiated condition showed no change in composition of the grain boundary, as expected.

A series of post-irradiation anneals were carried out at temperatures between 350 and 500°C for times ranging 0.5 to 35 hours. Hardness was measured for each annealing condition and is shown in Table 1 along with the value as a percent of hardening of the 360°C:1 dpa reference condition. This condition is also important because it is known to produce IASCC in constant extension rate tests in normal BWR water chemistry at 288°C. Heat treatments at 623K and 673K show promise in approximating the hardness of this condition. These heat treatments, as well as the irradiated condition, will be analyzed via TEM upon availability of the JEOL-2010F.

A second irradiation duplicating the conditions of the first is under way. TEM and SCC bars will be irradiated. Three conditions; as-irradiated, annealed 623K, and annealed 673K for the times listed in table 1, will be tested in constant extension rate tests in normal BWR water chemistry at 288°C. Optimization of irradiation and heat treatment will be conducted in Phase 3 and initial SCC susceptibility in Phase 4 of the project.

References

1. A. Jacobs and S. Dumbill, Proceedings of the 7th Env. Deg, NACE International, Houston, TX, 1995, 1021.
2. K. Asano et al., Proceedings of the 7th Env. Deg, NACE International, Houston, TX, 1995, 1033.
3. R. Katsura et al., Corrosion 98, Paper No. 132 (1998).
4. T. Allen, Ph.D. Dissertation, University of Michigan, 1996.
5. Perks et al., Proceeding of the symposium on radiation-induced sensitization of stainless steels, Berkeley, Glouchestershire, 1987, p 16-34.

Table 1. Hardness increase in irradiated and irradiated+annealed CP 304L SS

Condition	ΔH_v (kg/mm ²)	Relative Hardness
Ref. condition: 1.0 dpa:633K	60	1.0
As-irradiated	85	1.42
As-irrad + 3.8 hr @ 623K	66	1.09
As-irrad + 0.5 hr @ 673K	35	0.59
As-irrad + 0.5 hr @ 733K	27	0.45
As-irrad + 0.5 hr @ 773K	23	0.36

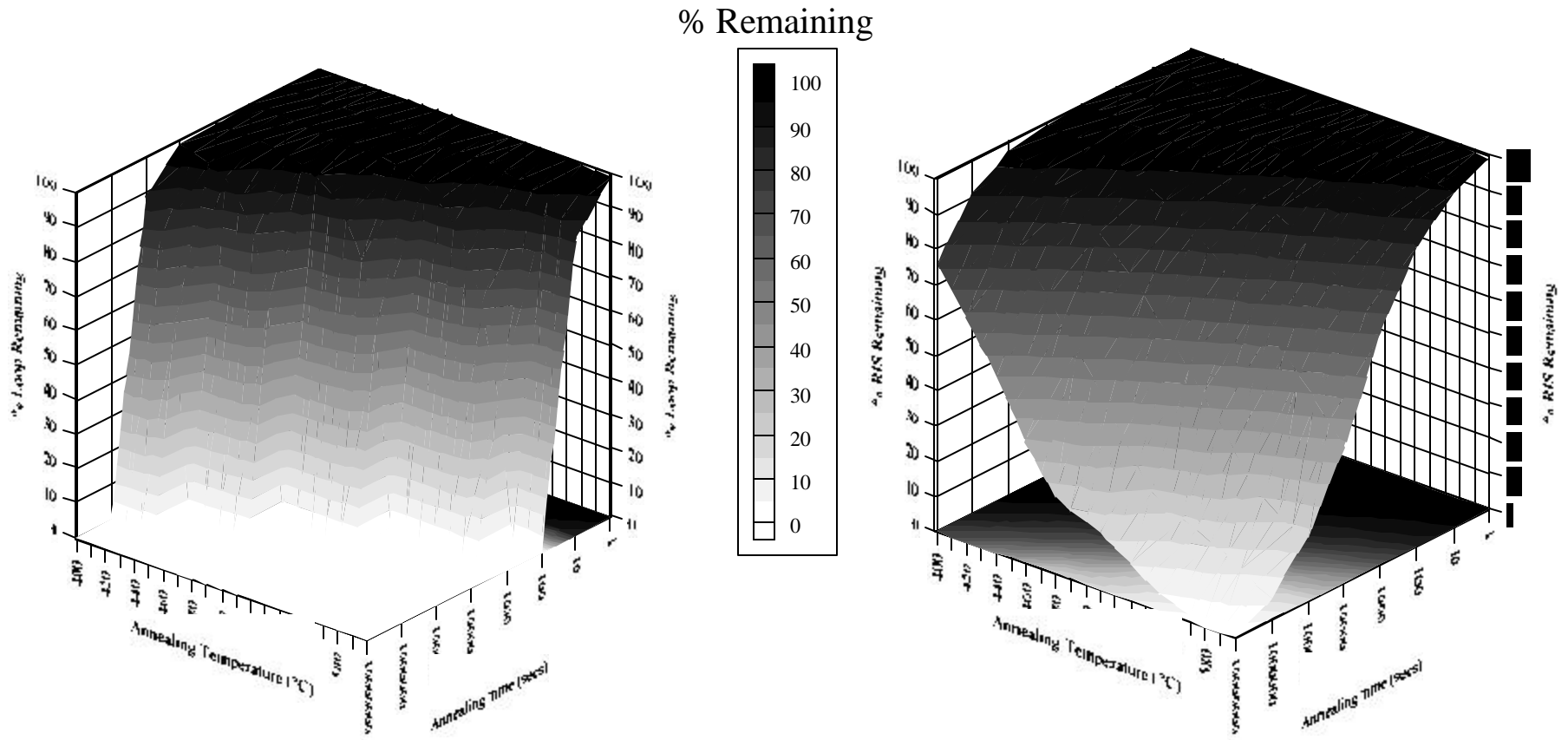


Figure 1: Annealing simulations of dislocation loops (left) and RIS (right) over a wide range of times and temper

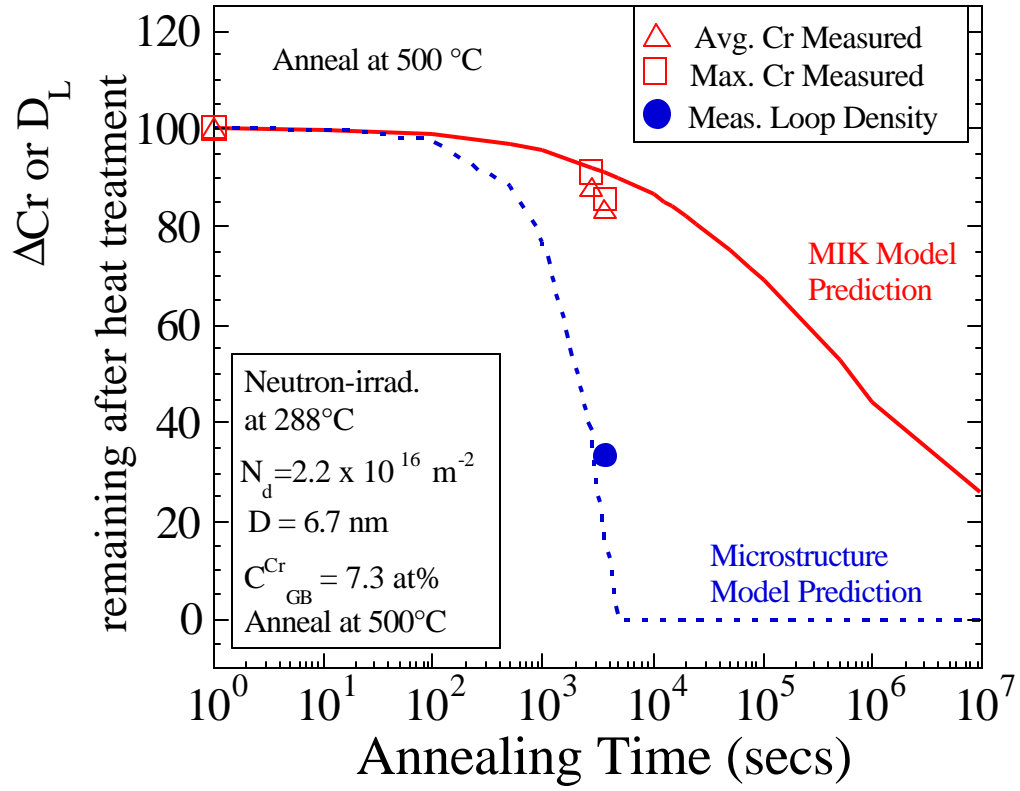


Figure 2: Comparison of microstructure and microchemical annealing simulations with existing experimental data¹ on grain boundary chromium depletion, ΔCr and dislocation line length, D_L remaining after annealing.

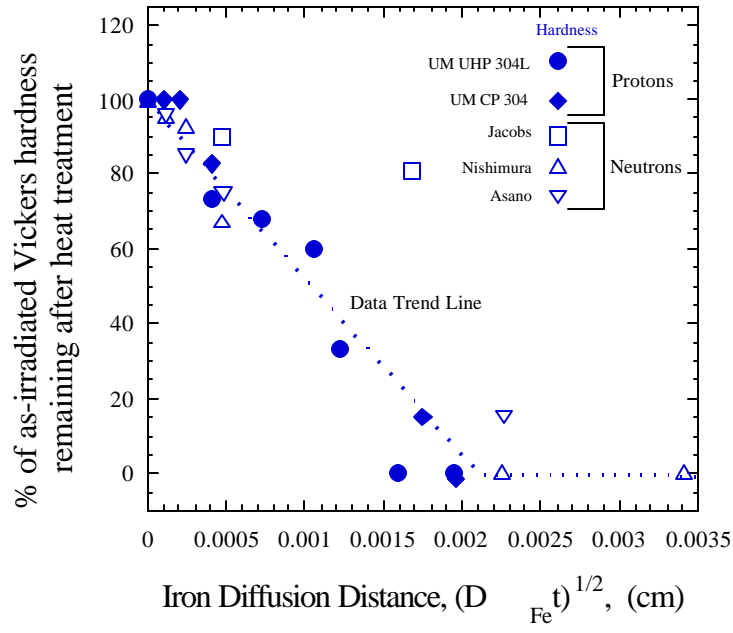


Figure 3: Comparison of changes in hardness in HP-304L and CP-304 during annealing with existing experimental data.

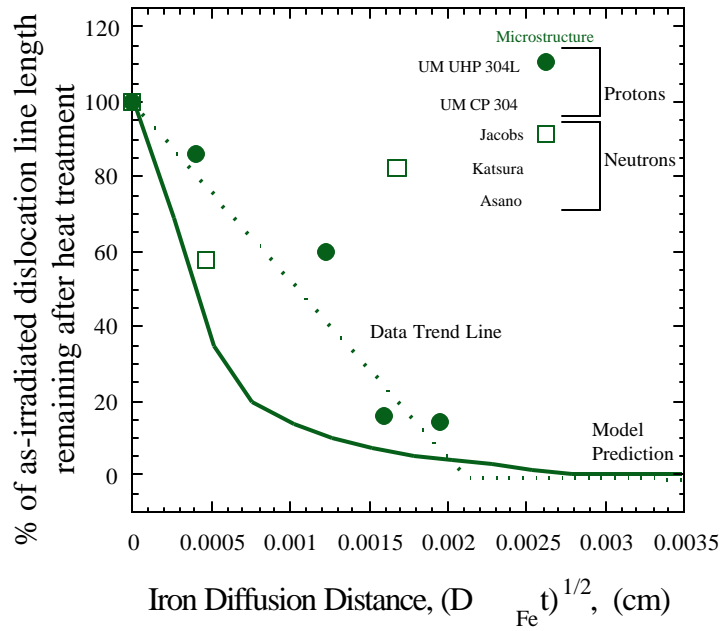


Figure 4: Comparison of changes in dislocation line length in HP-304L and CP-304 during annealing with existing experimental data and model predictions.

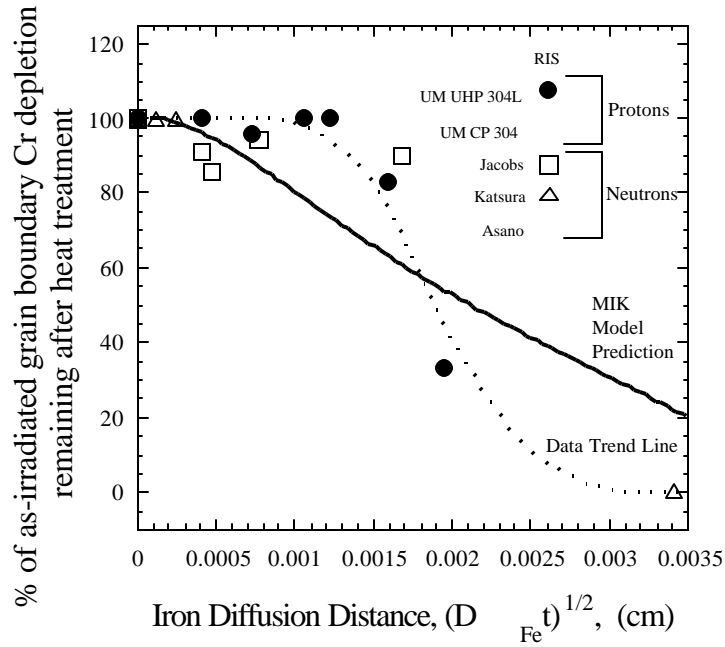


Figure 5: Comparison of changes in grain boundary Cr in HP-304L and CP-304 during annealing with existing experimental data and model predictions.

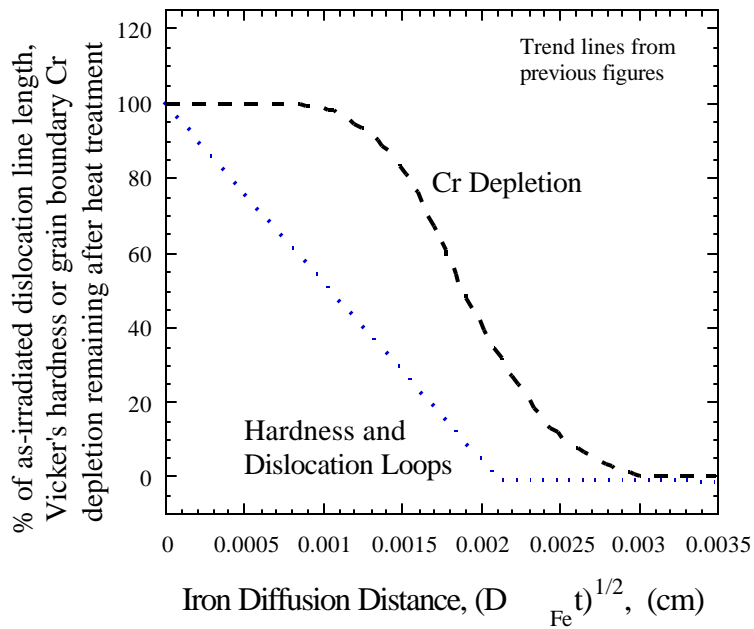


Figure 6: Comparison of trend line data changes in hardness, microstructure, and grain boundary Cr.